Environmental Science
Processes & Impacts

Accepted Manuscript

ROYAL SOCIETY OF CHEMISTRY

rsc.li/process-impacts

Environmental Impact

Little is currently known about the sources of airborne nanoparticles during summertime hot, arid and dusty climatic conditions in the Middle East region. This is a first *source apportionment* study for the airborne nanoparticles in this region that has quantified the contribution to particle number concentrations from numerous major sources, along with determining particle number distribution profiles of individual sources. Besides policy makers and environmental authorities findings of this work study could be important for modelling community to treat major nanoparticle sources in dispersion modelling and health impact assessments in the region.

Source apportionment of airborne nanoparticles in a Middle Eastern city using positive matrix factorization

Abdullah N. Al-Dabbous[a] *and Prashant Kumar*[a, b,*]

[a]*Department of Civil and Environmental Engineering, Faculty of Engineering and Physical Sciences (FEPS), University of Surrey, Guildford GU2 7XH, United Kingdom*

[b]*Environmental Flow (EnFlo) Research Centre, FEPS, University of Surrey, Guildford GU2 7XH, United Kingdom*

ABSTRACT

Airborne nanoparticles have been studied worldwide, but little is known about their sources in the Middle East region, where hot, arid and dusty climatic conditions generally prevail. For the first time in Kuwait, we carried out size-resolved measurements of particle number distributions (PNDs) and concentrations (PNCs) in the 5–1000 nm size range. Measurements were made continuously for 31 days during the summer months of May and June 2013 using a fast–response differential mobility spectrometer (Cambustion DMS500) at a sampling rate of 10 Hz. Sources and their contributions were identified using the positive matrix factorization (PMF) approach that was applied to the PND data. Simultaneous measurements of gaseous pollutants (i.e., O_3, NO, NO_x, SO_2 and CO), PM_{10}, wind speed and direction were also carried out to aid the interpretation of the PMF results through the conditional probability function plots and Pearson product-moment correlations. Six major sources of PNCs were identified, contributing ~46% (fresh traffic emissions), 27% (aged traffic

*Corresponding author: Address as above. Tel. +44 1483 682762; fax: +44 1483 682135;

Email addresses: P.Kumar@surrey.ac.uk, Prashant.Kumar@cantab.net (Dr Prashant Kumar)

emissions), 9% (industrial emissions), 9% (regional background), 6% (miscellaneous sources) and 3% (Arabian dust transport) of total PNCs. The sources of nanoparticles and their particle number distribution profiles identified could serve as a reference data to design more detailed field studies in future and treat these sources in dispersion modelling and health impact assessment studies.

Keywords: *Positive matrix factorization; Particle number size distribution; Source identification; Summertime nanoparticles; Middle East region*

1. Introduction

Exposure to particulate matter (PM) is known to adversely affect human health.[1] Ambient concentrations of PM are currently regulated through mass–based standards of PM_{10} and $PM_{2.5}$, i.e., aerodynamic diameters less than 10 and 2.5 μm, respectively.[2] Because of possessing negligible mass compared to the regulated PM,[3, 4] these standards do not control airborne nanoparticles that are referred to as those below 300 nm in diameter and represent the majority (~99%) of total particle number concentrations, PNCs.[5] Nanoparticles are characterised by their vast numbers and high surface area.[6, 7] As a result, they can adsorb large concentrations of toxic hazardous chemicals on their surfaces, translocate and deposit in different parts of the human body and thereby causing adverse health effects.[8, 9] Evidences from a large number of studies link the exposure of nanoparticles to the occurrence of cardiovascular diseases.[8] This effect is attributed to the translocation of the redox-active components of the nanoparticles in the human body, which promotes the progression of atherosclerosis.[10] Furthermore, preliminary estimates of excess mortality related to nanoparticle exposure have been reported to be notable at 11,252 deaths in 2010 in Delhi[11] and ~310,000 deaths per year in Asian megacities.[9] However, such estimates are currently

unavailable for the Middle East region, clearly showing a need for field studies that can provide an in-depth insight into the sources of nanoparticles and associated health impacts.

Pollutants measured at a receptor site are a combination of various local and regional sources situated at varying distances from a site. Nanoparticles are dynamic in nature with a potential to change in the atmosphere through transformation processes such as dilution, nucleation, coagulation, condensation/evaporation and deposition during their transport from the source to the receptor site.[12, 13] However, majority of the transformation occurs close to the source and the particle number distributions (PNDs) may not change considerably at large distances from their original emission source such as road traffic and petroleum refineries.[14, 15] Hence, the application of source apportionment models on the data collected at a receptor site could allow the extraction of the latent factors contributing to the total PND data and potentially reveal the nearby or faraway sources, along with their individual PND profiles. Our previous study[16] showed different PND profiles during variable wind directions at different times of the day, thereby representing the contribution of different sources to the measured size-resolved PND data. What remains unknown is the contribution of these different sources to the PNCs and the PND data collected during hot and arid weather conditions. These unstudied aspects are taken up for a detailed investigation in this study.

Source apportionment models are important to identify various unknown sources and quantify their contributions towards the total measured concentrations. Such information is important to design efficient abatement strategies to control emissions. One of the most common receptor–based source apportionment models is positive matrix factorization (PMF), which can overcome the drawbacks of principle component analysis, PCA.[17, 18] The output of PMF is more physically realistic than that of PCA because the former allows the implementation of non–negative constraints and production of explainable positive elements

among all factors. Other models such as the chemical mass balance (CMB) and Unmix are comparable to PMF, to some extent. However, PMF does not require prior knowledge of the sources and their profiles, as required in the case of CMB, thereby making it an easier and more cost-effective solution. Furthermore, PMF allows for the weighting of each data point individually[18] – a feature that is not available in the Unmix model.

Prior to the incorporation of PND data in the PMF, this source apportionment technique has been applied for the identification of particles sources in many previous studies.[19-22] However, these studies have mainly focused on PM mass concentrations and compositional data. PMF analysis, based on the PM chemical composition data, is often time-consuming and expensive, and does not segregate PNDs according to their sources. The knowledge of source-specific PNDs is of great relevance to epidemiological studies because of the size-dependency of respiratory tract deposition pattern in the human body on particle diameter.[23] Several studies worldwide have successfully deployed total PNC data in the application of PMF to identify sources and their contributions over the past decade (see summary of relevant studies in Table 1). Few of these studies have used only PND data for the PMF analysis,[24] while others have included PM chemical composition data,[25] gaseous pollutant data,[26] and chemical composition and gaseous pollutant data[15] in their PMF analysis. In fact, none of the studies till date have applied PMF to the distinct PND characteristics found in the Middle East region, and therefore, the contributions of the different sources of PNC are currently unknown.

In order to fill the above–noted research gaps, we have applied PMF to our PND data set, ranging from 5–1000 nm, collected continuously over a 31-day period during summertime conditions at a roadside location in Fahaheel, Kuwait, by using a fast response differential mobility spectrometer (Cambustion DMS500). In addition, PM_{10}, gaseous pollutants (NO_x,

O_3, CO and SO_2) and meteorological data were used to assist the interpretation of the PMF results by using conditional probability function (CPF).

The following are the unique features of our work. Firstly, the use of DMS500 is advantageous because it can provide real–time measurements of nanoparticles at a sampling rate of 10 Hz, allowing for the rapid capture of the fast transformation processes. The DMS500 is currently one of the commercially available fastest response particle sizers, requiring only ~100 ms to complete one full spectrum of PND. This enabled us to capture the peaks of PNCs that occur within a few seconds in urban environments.[27] Furthermore, the sampling height of the DMS500 inlet was ~1.60 m above the ground, representing the typical breathing height of the people, which can be easily used in epidemiological studies in calculating deposition doses. Secondly, the application of PMF was applied at a high temporal resolution (5–min based measurements), which is higher than that in most of the previous work (see Table 1), and on a continuous measured data of all studied parameters as opposed to the intermittent data used by some of previous studies (Table 1). Thirdly, most of the published work has only used wind direction in their CPF application (Table 1), but our study used both wind direction and speed, providing a better understanding of the directionality and position of the potential sources. Finally, to the best of our knowledge, this is a first instance when a source apportionment technique is used on high-resolution PND data in Kuwait, and the Middle East in general, which was collected during severe summertime conditions (maximum temperature ~48 °C and minimum relative humidity ~0.20%) with frequent dust events (Section 2.1).

In the light of the existing research gaps, the aims of this study are: (i) to identify the possible sources of nanoparticles in the studied area which represents a typical roadside environment

of the Middle East region, (ii) to quantify the sources contribution to total PNCs and (iii) to determine the individual PND spectrum of various sources in a Middle Eastern city, Kuwait.

2. Experimental methods

2.1 Site description

This study was conducted at a near–road location in the urban area of Fahaheel, Kuwait (Figure 1). The geographic coordinates of the sampling site are 29°4'52.70" N and 48°6'52.08" E. The sampling instruments were placed inside an air-conditioned cabin, located at a distance of ~15 m east of the kerbside of Fahaheel highway. This highway runs in the north–south direction, linking The State of Kuwait with the Kingdom of Saudi Arabia. This six-lane highway is one of the busiest highways in Kuwait, consisting of three lanes (~3.70 m wide) in each direction. These lanes are separated by a paved median strip, and there are two additional lanes in each direction reserved for emergency. The areas to the immediate east and west of the sampling site are intra–city activities and open flat desert, respectively. The intra–city activities in Fahaheel area consist of vehicular movement, gas stations and small businesses. Additionally, the sampling site is influenced from south–east direction by a vast range of petroleum, petrochemical, cement, caustic and small industries, located at a distance of 1200 m from the edge of these petroleum activities.[36]

Measurements were made during summertime in the month of May and June 2013 when ambient temperature reached to ~48 ºC, the relative humidity decreased to a minimum of 0.20% and the dust events (i.e., when PM_{10} >200 μg m^{-3}) were observed for ~49% of the total measurement time. The average temperature, relative humidity and wind speed were found to be 37±4.5 °C, 13.6±10.0% and 6.3±3.0 m s^{-1}, respectively. The prevailing wind direction was north-west (~311°N). Wind speed and ambient temperature affected the PNCs

notably. For example, ambient temperature was found to linearly decrease the PNCs due to partial evaporation[16]; see details in Supplementary Information, SI, Section S1.

The sampling site and the Fahaheel area are ideal for this study because of the following reasons. Firstly, Fahaheel is a typical urban area in Kuwait surrounded by heavy petroleum industries, reflecting typical characteristics of the oil–rich State of Kuwait and the intra-city activities, as well as is a good representative of the Middle East region (especially the Arabian Peninsula region), in terms of topography and climatic conditions. Secondly, no other major highways directly influence the sampling site, except the studied Fahaheel highway, allowing a clear identification of the highway impact on the measured PND data. Thirdly, the sampling site is characterised by the absence of obstacles for at least ~300 m radius, eliminating the downwash effects. Finally, the surrounding potential sources of the sampling site are well–distributed at different directions and distances, allowing the development of CPF plots using local wind data to aid in the source identification by PMF. Further details on the sampling site characteristics, including traffic and meteorology, can be seen in Al-Dabbous and Kumar[16].

2.2 Data acquisition

A total of 8675 valid 5–minute PND observations, each in 36 size classes, covering 5–1000 nm size range, were continuously measured from 27 May to 26 June 2013 by using a DMS500. These measurements were collected at 0.10–second time resolutions and then averaged to 5–min interval means to synchronise them with the pollutants and meteorological data. DMS500 is a parent version of DMS50 (i.e., portable instrument with similar features) that has been successfully used in a variety of our studies, related to roadside and kerbside measurements,[16, 37] vehicle-wake,[38] vehicle in-cabin[39-41] and indoor construction environments.[42, 43] The DMS500 detects particles based on their electrical mobility.[3] Additionally, a suite of pollutants (PM_{10}, O_3, NO_x, SO_2 and CO) and meteorological

parameters (temperature, relative humidity, wind speed and direction) were obtained from the adjacent (~300 m away from site) Environmental Protection Agency (EPA) monitoring station. These continuous data are well-maintained and quality-controlled by the Kuwait EPA. Further details on the experimental setup, instrumentation and working principle of various instruments can be seen elsewhere.[16]

2.3 Statistical analysis

PMF analysis was applied using the US EPA's PMF program (version 5.0) on the dataset composed of 36 variables. These variables included PNDs in 36 size classes covering a size range of 5–1000 nm, following the methodology described in Paatero[18]. PMF is a multivariate factor analysis model used to identify the contribution and profile by exposing the dataset to a multi-linear engine algorithm and a gradient algorithm approach in order to find the best-fit solution.[44, 45] This method is featured by the non–negative constraints and the use of uncertainties to scale individual data points. The uncertainty data file supplied by the instrument manufacturer (Cambustion Ltd., Cambridge), consisting of size–specific minimum detection limits and error fractions, was also included in the PMF. An extra modelling uncertainty of 5% was added to the model to account for any additional measurement errors that were not covered by the uncertainty data file.[46] The missing sampling values due to instrument failure were modest (i.e., <3% of the entire sampling period) and simply excluded from the analysis. In addition, CPF plots were prepared using the threshold of the upper 25th percentile of the fractional contribution of each factor/source. These plots complemented the PMF analysis by depicting the trend in the factors score with wind direction and speed so that factors could be tentatively assigned to the potential sources in the area.[47] Furthermore, CPF plots were also drawn for the routinely measured pollutants (PM_{10}, O_3, NO_x, SO_2 and CO) by using the same criterion. Open Air (R package), which is an

open-source statistical tool,[48] was used to derive the CPF plots that assisted in the interpretation of the measured air pollution data.

3. Results and discussion

Using the PMF approach described in Section 2.3, six different factors were identified that were then tentatively assigned to the potential sources based on the following information: (i) factor-specific PNDs (Figure 2 and Figure 3g-l, middle vertical panel), (ii) diurnal variation of the factors (Figure 3m-r, right vertical panel), (iii) contribution of each factor to the total PNC (Figure 4), (iv) hourly Pearson product–moment correlations, along with the significance level (p-value), between each factor contribution and measured gaseous (O_3, NO_x, SO_2 and CO) and PM_{10} pollutants (Table 2), and (v) the CPF plots for each factor contribution (Figure 3a-f, left vertical panel) and measured gaseous (O_3, NO_x, SO_2 and CO) and PM_{10} pollutants (Figure 5).

3.1 Factor 1: Miscellaneous sources

This factor showed multiple PND modes, with the major peaks at about 365 nm and 1000 nm, and a positive correlation with PM_{10} ($r = 0.39$; p-value <0.01; Table 2). Factor 1 also showed a minor peak at ~5 nm, which could represent fresh traffic emissions but to lesser extent than that observed for factors 4 and 5. Furthermore, the wind directionality and the relatively high wind speed (up to 10 m s^{-1}) of this factor (Figure 3a) and PM_{10} (Figure 5a) indicated that the particle emissions had travelled from a remote location and grown to larger sizes through coagulation. Al-Dabbous and Kumar[16] previously reported a dominating role of PM_{10} in suppressing PNCs due to coagulation process. For instance, PNCs were found to be reduced by ~23% when PM_{10} concentration increased by ~500%, compared to the values prior to the arrival of the dust event (i.e., when PM_{10} <200 μg m^{-3}). A similar observation on coagulation scavenging has been reported by Jayaratne *et al.*[49] with respect to the influence

of the Australian dust storm on the PNCs. This factor made the second lowest contribution (6%) to the total PNCs. The directionality of the CPF plots and the association with PM_{10} clearly corresponds to the west Shuaiba industrial area and the dust blown by high wind speed from the desert during the south-westerly winds.

Furthermore, particles emitted from the industrial area appears to be aged particles that have spent time in the atmospheric environment and grown to larger sizes during their travel from their far sources (for example, west Shuaiba industrial area during the south westerly winds, in this case). These particles could be attributed to the vehicle movements within the industrial area such as those found in Factor 5 (Section 3.5), but neither the factor contribution did show any nocturnal variation (Figure 3m) nor the PND profile (Figure 3g) and the poor correlations with the NO_x and CO (Table 2) support any direct association with the traffic emissions. For example, the diurnal behaviour of factor 1 (Figure 3m) showed a slight drop in factor contribution during the afternoon hours; otherwise this remains fairly constant during the rest of the period. The reason for this slight drop could be attributed to the unstable atmospheric conditions, induced by the intensive solar radiation (800±548 W m^{-2} during the afternoon hours compared with an average value of 323±373 W m^{-2} during the entire period), leading to relatively larger mixing of these particles.[16] Although this factor was tentatively assigned to shared sources, information available from the correlations between factor contribution and gaseous pollutants (Table 2), and diurnal profile of factor contribution (Figure 3m), was insufficient to assign a separate weighting to each of these two different sources.

3.2 Factor 2: Arabian dust transport

This factor showed a bimodal PND (Figure 3i) with a major peak at 560 nm, and a minor peak at 60 nm, along with a distinctively high correlation with PM_{10} ($r = 0.71$; p-value <0.01; Table 2). The wind directionality and the associated high speed levels (more than 15

m s^{-1}) noted in CFP plots of this factor (Figure 3b), as well as PM_{10} (Figure 5a), indicate the influence of the dust from the long–range transport that is associated with the typical Arabian dust events. This factor showed behaviour similar to that of factor 1, but to a greater extent in terms of higher PM_{10}, wind speed levels and the typical directionality (i.e., north–westerly direction) associated with the frequent dust events in the region. In an extended analysis of the same dataset,[16] Arabian dust events were found to suppress PNCs due to the influence of coagulation process, which explains the minimum contribution (3%) of this factor to the total PNC (Figure 4). It is worth pointing out that both the factors 1 (6%) and 2 (3%) made the lowest contributions (Figure 4), among the six resolved factors, but showed the highest correlations with PM_{10}; these characteristics support the possible effects of the coagulation process during high concentrations of PM_{10} approaching the site from the westerly wind direction (i.e., open desert; Figure 1). Furthermore, the diurnal profile of this factor showed an increased contributions during the afternoon (12:00 to 14:00 h; Figure 3n) due to relatively higher wind speeds and associated saltation process.[50] In an extended analysis on the same dataset (SI Figure S1), but excluding the major dust event periods (i.e., when PM_{10} >1000 μg m^{-3}), we observed almost similar contribution to the total PNCs (Figure S2) to those observed in Figure 4 for all the six sources. Pearson product–moment correlations between each factor and measured gaseous (O_3, NO_x, SO_2 and CO) and PM_{10} pollutants also exhibited similar correlations (Table S1) to those observed in Table 2. This similarity confirms that the input dataset were not highly affected by the Arabian dust events, mainly because the major dust event periods were only 5.7% of the total measurements period.

3.3 Factor 3: Industrial emissions

This factor showed a monomodal distribution with a peak at ~42 nm (Figure 3i), and made a 9% contribution to the total PNCs (Figure 4). The diameter of this peak was in accordance with those recorded for industrial emissions in previously published studies. For

instance, Ogulei *et al.*[31] reported a peak at 44 nm during their one–year long measurements (2004–2005) at an urban background location in New York (USA) that was significantly influenced by the industrial activities. We have several reasons to believe that factor 3 represents industrial emissions. For example, the CPF plots of this factor are strongly associated with south easterly winds (Figure 3c), which is consistent with the wind directionality of SO_2 (Figure 5b). The directionality of these plots clearly correspond to the Shuaiba industrial area, which hosts a range of oil refineries (i.e., Mina Al-Ahmadi, Shuaiba and Mina Abdullah refinery), petrochemical industries (e.g., ammonia, urea, polyethylene and polypropylene plant) and two power desalination plants.[51, 52] Furthermore, this factor had the highest correlation ($r = 0.31$; p–value <0.01) with SO_2 among all the factors (Table 2), which supports the fact that industrial emissions are clearly associated with this factor. Moreover, NO_x ($r = 0.37$; p-value < 0.01) and CO ($r = 0.23$; p-value <0.01) also showed a positive correlation with this factor, indicating an association with the combustion activities within the vicinity of the industrial area. Past studies have also linked industrial emissions with the combustion related pollutants, mainly SO_2.[29, 31, 33, 35] The association with SO_2 may indicate the influence of secondary particle formation in the form of photo-chemically induced sulphuric-acid nucleation.[53, 54] The diurnal profile of this factor displayed a typical diurnal variation, linked with the meteorological conditions and the associated boundary layer [55]. For example, a decreased factor contribution was observed during the afternoon, which was caused by the expanded depth of the boundary layer and the associated dilution with the background air. Based on the above concluding evidences, we attributed this factor to the industrial emissions.

3.4 Factor 4: Fresh traffic emissions

This factor showed a major PND peak between 5–12 nm and another minor peak at ~60 nm (Figure 3j) and explained nearly half (46%; Figure 4) of the total PNC contribution.

Looking at the PND and the peaks, this contribution was believed to be from the local traffic. For example, this bimodal profiles of PNDs are consistent with those observed by Fujitani *et al.*[56] at 10 nm and 40–60 nm during their near road measurements in Kanagawa Prefecture, Japan. Furthermore, similar PND peaks related to local traffic were observed by numerous studies performed in cities worldwide, such as at 20 nm (major peak) and 100 nm (minor peak) in Beijing, China,[15] 20 nm in Brisbane, Australia,[28] 9–40 nm in Augsburg, Germany,[25] 10–100 nm in Erfurt, Germany,[24] 20 nm in London, UK,[26] 13.3 nm in Cambridge, UK,[5] 10 nm in New York, USA,[31] 15 nm in Pittsburgh, USA.[35] The wind directionality (Figure 3d) corresponded to the highway located at 15 m west of the measurement location, and the wind speed was observed to be relatively low (<5 m s^{-1}) compared with much higher levels noted during the major dust events. This low level of wind speed indicates an association with close-range source (i.e., local traffic). The directionality of the factor contribution is also consistent with those for NO_x (Figure 5c) and CO (Figure 5d), especially from the westerly wind direction, indicating the same emission source. Furthermore, this factor contribution correlated positively with the NO_x ($r = 0.30$; p-value <0.01), which is a primary traffic–generated pollutant.[57, 58] The diurnal profile of this factor contribution (Figure 3p) was in agreement with the diurnal pattern of the traffic volume, except during the noon hours when the high traffic volume corresponded to low factor contribution. The reason for this odd behaviour was previously studied in an extended analysis by Al-Dabbous and Kumar[16] and explained by the extreme temperature (reaching up to ~50 °C) that resulted in partial evaporation and increased rate of coagulation with larger particles.[59] Most of the above-discussed studies also observed higher PND magnitude in the morning rush hours compared with those during evening rush hours; this is consistent with the findings of our current study. Based on the above observations, we attributed this factor to local traffic emissions, seen through the newly formed particles (i.e., fresh traffic emissions) in nucleation mode.

3.5 Factor 5: Aged traffic emissions

This factor showed a major peak at 24 nm, followed by a minor peak at 130 nm (Figure 3k). The former peak is presumably attributed to the nearby highway emissions, and the latter, to aged particles transported from the industrial area. These bimodal profiles of PNDs are similar to those observed by Gu *et al.*[25] at 20 and 100 nm during their measurements in Augsburg, Germany, and attributed them to aged traffic emissions. This factor showed the second highest contribution to the total PNC (27%; Figure 4). This factor was positively correlated with NO_x ($r = 0.54$; p-value <0.01) and CO ($r = 0.23$; p-value <0.01) and showed no correlation with SO_2. Moreover, the CPF shown in Figure 3e clearly pointed out the wind direction from the Shuaiba industrial area (i.e., south-easterly direction) and the traffic emission from Fahaheel highway (i.e., westerly direction). This wind directionality is identical to those obtained for NO_x (Figure 5c) and CO (figure 5d). Therefore, the correlations with the NO_x and CO as well as the CPF suggest that there is a contribution from *primary* (solid carbonaceous) particles from diesel vehicles from the nearby industrial area and the Fahaheel highway. However, absence of such correlations with the SO_2 suggests a negligible contribution of *secondary* particle formation through photo–chemically induced sulphuric–acid nucleation like what is noticed in case of factor 3. Furthermore, the diurnal profile of this factor contribution (Figure 3q) was similar to the profile of factor 4, with a slight increase in the evening hours, indicating the influence of nocturnal commercial traffic (e.g., heavy duty trucks) operating on the Fahaheel highway and within the industrial area. In total, both the fresh (factor 4) and aged (factor 5) traffic emissions accounted for about 73% of the total PNCs, which is comparable to roadside studies in London, UK (~72%)[26] and Brisbane, Australia (~74%)[28].

3.6 Factor 6: Regional background

This factor showed multiple PND peaks with a major peak at 150 nm, followed by a minor peak at 750 nm (Figure 3l), and contributed to 9% of the total PNCs (Figure 4). Particles in the size range (diameter >100 nm) could possibly be originated: (i) either locally, through direct emissions from local sources such as exhaust emissions or brake dust, or coagulation of smaller particles with each other and with their larger counterparts,[3] or (ii) regionally that are transported to the receptor site.[29] However, the wind directionality shown in Figure 3f indicate that the PNC emissions were approaching to the site from all the wind directions and the association with the high wind speed indicated a contribution from the far–range sources. Particles larger than 100 nm contain low volatility and solid cores.[23] Therefore, these can travel relatively larger distances compared with highly volatile nucleation mode particles[12, 60]. This factor also showed the highest correlation with PM_{10} ($r = 0.31$; p-value <0.01) compared with other pollutants (Table 2), agreeing with those reported by Ogulei *et al.*[31] where they found a high correlation with regionally transported $PM_{2.5}$. Both the factors 6 and 1 showed identical correlations with the PM_{10}, but information available from the wind directionality and PNDs profile assist in attributing the factor 6 to regional background. Furthermore, the lack of obvious diurnal variation in factor contribution (Figure 3r) also suggests that this is a regional background source.

4. Summary and conclusions

Particle number and size distributions in the size range of 5–1000 nm were continuously measured for a period of one month, starting from 27 May to 26 June 2013, at a roadside location in Kuwait. The aims of the study were to identify the sources size-resolved particles under summertime climatic conditions, as well as with quantifying their contributions, and understanding their influencing parameters (PM_{10}, gaseous pollutants and meteorological parameters).

The application of PMF helped in identifying six probable sources: miscellaneous sources, Arabian dust transport, industrial emissions, fresh as well as aged traffic emissions, and regional background. Traffic emissions made the highest (73%) contributions to the total PNC, followed by industrial emissions (9%), regional background (9%), miscellaneous sources (6%) and Arabian dust transport (3%). The high correlations between PM_{10} and the factor contribution of the last three sources indicated the possible influence of coagulation of PNCs with their larger counterparts and thus resulting in the suppression of total PNCs. The diurnal profile of the factor contribution of the traffic sources (i.e., *factor 4* and *factor 5*) were categorised by a bimodal distribution, coinciding with the morning and evening rush hours, whereas Arabian dust transport (i.e., *factor 2*) was characterised by an increased factor contribution in the noon hours, where high wind speed approached the sampling site loaded with high levels of PM_{10}. Miscellaneous sources (*factor 1*) and regional background (*factor 6*) displayed no diurnal variation in their factor contribution, expect during noon hours where high dilution was expected due to the expanded boundary layer and the associated high wind speed. Traffic sources (i.e., *factors 4* and *5*) showed a typical bimodal PND, while all the long–range transport sources (i.e., *factors 1, 2,* and *6*) consisted mostly of particles greater than 100 nm in diameter, resulting from their growth in size during transport from sources far away. Industrial emissions (i.e., *factor 3*) displayed a unique monomodal PND, peaking at about 42 nm. The similarities in the wind directionality of the factors contribution and the pollutants, using CPF at 75^{th} percentile threshold criterion, assisted in sources allocation.

This study covers a hitherto overlooked topic in the Middle East region. The findings of this work make contributions towards the understanding of potential sources of nanoparticles in the area and their probable contribution to the PNCs. Furthermore, PND profiles associated with individual sources present an important reference data for future studies in the Middle East region. Long-term measurement studies, involving more pollutants (e.g., trace metals

and organic compounds), are recommended to elucidate further on specific source characteristics and their emission strengths.

5. Acknowledgements

The authors are grateful to the Kuwait Institute for Scientific Research (KISR) for experimental and funding support for Abdullah's PhD research. We also thank Professors Alan Robins (University of Surrey) and Min Hu (Peking University), and Drs Jianfei Peng (Peking University) and Jonathan Symonds (Cambustion Ltd) for their valuable contributions and discussion to develop this article. We also thank the Kuwait National Meteorological Network and Kuwait Environmental Protection Agency for their cooperation in providing us the meteorological and gaseous pollutants data.

6. References

1. WHO, *WHO Air quality guidelines for particulate matter, ozone, nitrogen dioxide and sulfur dioxide - Global update 2005 - Summary of risk assessment*, World Health Organization, Regional Office for Europe, 2006.

2. M. R. Heal, P. Kumar and R. M. Harrison, *Chem. Soc. Rev.*, 2012, 41, 6606-6630.

3. P. Kumar, A. Robins, S. Vardoulakis and R. Britter, *Atmos. Environ.*, 2010, 44, 5035-5052.

4. L. Morawska, Z. Ristovski, E. R. Jayaratne, D. U. Keogh and X. Ling, *Atmos. Environ.*, 2008, 42, 8113-8138.

5. P. Kumar, P. Fennell, D. Langley and R. Britter, *Atmos. Environ.*, 2008, 42, 4304-4319.

6. P. Kumar, L. Pirjola, M. Ketzel and R. M. Harrison, *Atmos. Environ.*, 2013, 67, 252-277.

7. B. Nowack, *Environ. Pollut.*, 2009, 157, 1063-1064.

8. HEI, *HEI perspectives 3: Understanding the health effects of ambient ultrafine particles (HEI review panel on ultrafine particles)*, Health Effects Institute, Boston, Massachusetts, 2013.

9. P. Kumar, L. Morawska, W. Birmili, P. Paasonen, M. Hu, M. Kulmala, R. M. Harrison, L. Norford and R. Britter, *Environ. Int.*, 2014, 66, 1-10.

10. R. J. Delfino, C. Sioutas and S. Malik, *Environ. Health Persp.*, 2005, 113, 934-946.

11. P. Kumar, B. R. Gurjar, A. S. Nagpure and R. M. Harrison, *Environ. Sci. Technol.*, 2011, 45, 5514-5521.

12. P. Kumar, M. Ketzel, S. Vardoulakis, L. Pirjola and R. Britter, *J. Aerosol Sci.*, 2011, 42, 580-603.

13. M. Carpentieri, P. Kumar and A. Robins, *Environ. Pollut.*, 2011, 159, 685-693.

14. E. Kim, P. K. Hopke, T. V. Larson and D. S. Covert, *Environ. Sci. Technol.*, 2004, 38, 202-209.

15. Z. Liu, Y. Wang, Q. Liu, B. Hu and Y. Sun, *Atmos. Chem. Phys. Discuss.*, 2013, 13, 1367-1397.

16. A. N. Al-Dabbous and P. Kumar, *Environ. Sci. Technol.*, 2014, 48, 13634-13643.

17. P. Paatero and U. Tapper, *Environmetrics*, 1994, 5, 111-126.

18. P. Paatero, *Chemometr. Intell. Lab.*, 1997, 37, 23-35.

19. E. Kim, P. K. Hopke and E. S. Edgerton, *J. Air Waste Manag. Assoc.*, 2003, 53, 731-739.

20. E. Lee, C. K. Chan and P. Paatero, *Atmos. Environ.*, 1999, 33, 3201-3212.

21. Z. Ramadan, X.-H. Song and P. K. Hopke, *J. Air Waste Manag. Assoc.*, 2000, 50, 1308-1320.

22. A. V. Polissar, P. K. Hopke and R. L. Poirot, *Environ. Sci. Technol.*, 2001, 35, 4604-4621.

23. W. C. Hinds, *Aerosol technology: properties, behaviour and measurement of airborne particles*, John Wiley & Sons, New York, 1999.

24. W. Yue, M. Stölzel, J. Cyrys, M. Pitz, J. Heinrich, W. G. Kreyling, H. E. Wichmann, A. Peters, S. Wang and P. K. Hopke, *Sci. Total Environ.*, 2008, 398, 133-144.

25. J. Gu, M. Pitz, J. Schnelle-Kreis, J. Diemer, A. Reller, R. Zimmermann, J. Soentgen, M. Stoelzel, H. Wichmann and A. Peters, *Atmos. Environ.*, 2011, 45, 1849-1857.

26. R. M. Harrison, D. C. S. Beddows and M. Dall'Osto, *Environ. Sci. Technol.*, 2011, 45, 5522-5528.

27. A. Goel and P. Kumar, *Atmos. Environ.*, 2014, 97, 316-331.

28. A. Friend, G. Ayoko, E. R. Jayaratne, M. Jamriska, P. Hopke and L. Morawska, *Environ. Sci. Pollut. Res.*, 2012, 19, 2942-2950.

29. J. Kasumba, P. K. Hopke, D. C. Chalupa and M. J. Utell, *Sci. Total Environ.*, 2009, 407, 5071-5084.

30. D. Thimmaiah, J. Hovorka and P. K. Hopke, *Aerosol Air Qual. Res.*, 2009, 9, 209-236.

31. D. Ogulei, P. K. Hopke, D. C. Chalupa and M. J. Utell, *Aerosol. Sci. Tech.*, 2007, 41, 179-201.

32. D. Ogulei, P. K. Hopke, A. R. Ferro and P. A. Jaques, *J. Air Waste Manag. Assoc.*, 2007, 57, 190-203.

33. D. Ogulei, P. K. Hopke, L. Zhou, J. Patrick Pancras, N. Nair and J. M. Ondov, *Atmos. Environ.*, 2006, 40, 396-410.

34. L. Zhou, P. K. Hopke, C. O. Stanier, S. N. Pandis, J. M. Ondov and J. P. Pancras, *J. Geophys. Res-Atmos. (1984–2012)*, 2005, 110.

35. L. Zhou, E. Kim, P. Hopke, C. Stanier and S. Pandis, *Aerosol Sci. Tech.*, 2004, 38, 118-132.

36. A. Al-Dabbous, A. Khan, M. Al-Rashidi and L. Awadi, *Indoor Built Environ.*, 2013, 22, 456-464.

37. A. N. Al-Dabbous and P. Kumar, *Atmos. Environ.*, 2014, 90, 113-124.

38. M. Carpentieri and P. Kumar, *Atmos. Environ.*, 2011, 45, 5837-5852.

39. P. Joodatnia, P. Kumar and A. Robins, *Atmos. Environ.*, 2013, 71, 364-375.

40. P. Joodatnia, P. Kumar and A. Robins, *Atmos. Environ.*, 2013, 65, 40-51.

41. A. Goel and P. Kumar, *Atmos. Environ.*, 2015, DOI: http://dx.doi.org/10.1016/j.atmosenv.2015.02.002.

42. F. Azarmi, P. Kumar and M. Mulheron, *J. Hazard. Mater.*, 2014, 279, 268-279.

43. P. Kumar and L. Morawska, *Atmos. Environ.*, 2014, 90, 51-58.

44. P. Paatero, S. Eberly, S. G. Brown and G. A. Norris, *Atmos. Meas. Tech.*, 2014, 7, 781-797.

45. G. Norris, R. Duvall, S. Brown and S. Bai, *EPA Positive Matrix Factorization (PMF) 5.0 Fundamentals and User Guide*, U.S. Environmental Protection Agency, Office of Research and Development Washington, DC, 2014.

46. A. Reff, S. I. Eberly and P. V. Bhave, *J. Air Waste Manag. Assoc.*, 2007, 57, 146-154.

47. L. L. Ashbaugh, W. C. Malm and W. Z. Sadeh, *Atmos. Environ. (1967)*, 1985, 19, 1263-1270.

48. D. C. Carslaw and K. Ropkins, *Environ. Modell. Softw.*, 2012, 27–28, 52-61.

49. E. R. Jayaratne, G. R. Johnson, P. McGarry, H. C. Cheung and L. Morawska, *Atmos. Environ.*, 2011, 45, 3996-4001.

50. V. Tsiouri, K. Kakosimos and P. Kumar, *Air Qual. Atmos. Health.*, 2014, DOI: 10.1007/s11869-014-0277-4, 1-14.

51. S. M. Al-Salem and A. R. Khan, *Int. J. Chem. Eng.*, 2010, DOI: 10.1155/2010/879836.

52. M. U. Beg, T. Saeed, S. Al-Muzaini, K. R. Beg and M. Al-Bahloul, *Ecotox. Environ. Safe.*, 2003, 54, 47-55.

53. M. Kulmala, H. Vehkamäki, T. Petäjä, M. Dal Maso, A. Lauri, V. M. Kerminen, W. Birmili and P. H. McMurry, *J. Aerosol Sci.*, 2004, 35, 143-176.

54. C. O'Dowd, G. McFiggans, D. J. Creasey, L. Pirjola, C. Hoell, M. H. Smith, B. J. Allan, J. M. C. Plane, D. E. Heard, J. D. Lee, M. J. Pilling and M. Kulmala, *Geophys. Res. Lett.*, 1999, 26, 1707-1710.

55. R. B. Stull, *An introduction to boundary layer meteorology*, Springer, 1988.

56. Y. Fujitani, P. Kumar, K. Tamura, A. Fushimi, S. Hasegawa, K. Takahashi, K. Tanabe, S. Kobayashi and S. Hirano, *Sci. Total Environ.*, 2012, 437, 339-347.

57. A. Can, M. Rademaker, T. Van Renterghem, V. Mishra, M. Van Poppel, A. Touhafi, J. Theunis, B. De Baets and D. Botteldooren, *Sci. Total Environ.*, 2011, 409, 564-572.

58. P. Kumar and B. Imam, *Sci. Total Environ.*, 2013, 444, 85-101.

59. M. Jacobson, D. Kittelson and W. Watts, *Environ. Sci. Technol.*, 2005, 39, 9486-9492.

60. M. Dall'Osto, A. Thorpe, D. Beddows, R. Harrison, J. Barlow, T. Dunbar, P. Williams and H. Coe, *Atmos. Chem. Phys.*, 2011, 11, 6623-6637.

List of figure captions

Figure 1. Location of the sampling site in the Fahaheel area, showing the major sources surrounding the site. Satellite image includes material ©NSPO 2014 distribution Spot Image S.A.; courtesy of Airbus Defence and Space, all rights reserved. Note: SIA = Shuaiba Industrial Area; WSIA = West Shuaiba Industrial Area.

Figure 2. Percent contribution of each source identified towards the PNCs in different size ranges.

Figure 3. Directionality of the factor contribution using CPF plots at 75th percentile level, considering both local wind direction and speed (Figure 3a-f). The colours in Figure 3a-f represent the probability of factor contribution with respect to wind direction and speed. Figures 3g-l represent the factor-specific PND profiles while Figures 3m-r show the diurnal variation of the normalised factor contribution.

Figure 4. Sources contribution (%) to the total PNC data in the urban area of Fahaheel, Kuwait.

Figure 5. Directionality of (a) PM_{10}, (b) SO_2, (c) NO_x, (d) CO and (e) O_3 using CPF plots at 75th percentile level, considering both local wind direction and speed. The colours in these figures represent the probability of the aforementioned pollutants with respect to wind direction and speed.

List of Tables

Table 1. Summary of recent PMF studies focusing on PND data set, together with other auxiliary parameters (e.g., gaseous pollutants, particulate matter, chemical composition and traffic).

Author (year)	Location (type)	Size range (nm)	Instruments	Additional data	Sources identified (contribution of each source to the total apportioned PNC, %)
This study	Fahaheel, Kuwait (roadside)	5–1000	DMS500	PM_{10} and Gaseous (O_3, NO, NO_x, SO_2 and CO)	Local traffic (46% of the total apportioned PNC), mixture of local traffic and industrial emissions (27%), industrial emissions (9%), regional background (9%), miscellaneous sources (6%), Arabian dust transport (3%)
Liu *et al.*[15]	Beijing, China (urban background)	14.5–2514	SMPS	Gaseous (O_3, NO, NO_2, CO and SO_2), and chemical composition (organic matter, sulphate, nitrate, ammonium and chlorine)	Local sources: cooking (22.8%), solid-mode exhaust (18.8%), nucleation-mode exhaust (18.7%), secondary nitrate (8.9%), secondary sulphate (7.9%), coal-fired power plant (6.8%) and road dust (2.3%) Regional sources: accumulation mode (13.8%)
Friend *et al.*[28]	Brisbane, Australia (roadside)	14–715	SMPS	PM_{10}, gaseous (CO, NO and NO_2)	Petrol vehicles (30.8%), diesel traffic (28.1%), local traffic (14.9%), biomass burning (20.1%) and two unidentified sources (6%)
Gu *et al.*[25]	Augsburg, Germany (urban background)	3–10000	UDMA, UCPC and APS	Metals, water-soluble ions, elemental carbon (EC) and organic carbon (OC)	Aged traffic (40.3%), re-suspended dust (32.6%), stationary combustion (26.1%), fresh traffic (24.9%), nucleation particles (3.7%), secondary aerosols (1.2%), and long-range transported dust (1.1%)
Harrison *et al.*[26]	London, UK (curbside)	15–10000	SMPS and APS	Gaseous (O_3, NO, NO_2 and CO) and traffic flow	Road emissions: solid-mode exhaust (18.8%), brake dust (13.7%), re-suspended dust (4.4%) and nucleation-mode exhaust (3.6%) Urban background: well-aged regional (26.8%), accumulation mode (12.8%), solid fuel/nitrate (8.4%), cooking (6.7%), regional (2.5%) and suburban traffic (2.3%)
Kasumba *et al.*[29]	New York, USA (urban background)	100–470	SMPS	$PM_{2.5}$ and gaseous (CO, SO_2 and O_3)	Local traffic or gasoline traffic (21.7%), mixture of nucleation and traffic (20.1%), industrial emissions (17.2%), distant traffic or diesel traffic (15.2%), nucleation (17.6%), secondary sulphate (6.4%), ozone-rich secondary aerosol (0.9%), and regionally transported aerosol (1.1%)
Thimmaiah *et al.*[30]	Prague, Czech Republic (urban background)	18.8–723.5	SMPS	Gaseous (CO, SO_2, NO_x, O_3, CH_4, Non Methane Hydrocarbons	NO_x-rich (influenced by diesel emissions, 37.8%), gasoline traffic (34.2%), heating (24.6%) and ozone-rich (mainly influenced by meteorology, 3.5%)

				and Total Hydrocarbons	
Yue *et al.*[24]	Erfurt, Germany (roadside)	10–3000	MAS	Gaseous (O_3, NO, NO_2, CO and SO_2) and Chemical composition (sulphate, EC and OC)	Ultrafine particles from local traffic (79%), secondary aerosols from multiple sources (6%), particles from remote traffic sources (5%) and airborne soil (1%)
Ogulei *et al.*[31]	New York, USA (urban background)	10–470	SMPS	$PM_{2.5}$, gaseous (CO, SO_2 and O_3)	Diesel/distant traffic (23.3%), mixture of gasoline/local traffic and nucleation (22%), industrial emissions (21.4%), nucleation (15.7%), secondary sulphate (10.9%), ozone-rich secondary aerosol (4.7%) and regionally transported aerosol (1.9%)
Ogulei *et al.*[32]	New York, USA (on-road, mobile)	6–500	EEPS	--	Background urban emissions (39.5%), local/street diesel traffic (21.2%), aged/evolved diesel particles (15.5), fresh tail-pipe diesel exhaust (15.4%), spark-ignition gasoline emissions (4.3%) and secondary/transported material (4%)
Ogulei *et al.*[33]	Baltimore, USA (roadside)	9.6–2458	SMPS and APS	$PM_{2.5}$, Gaseous (O_3, NO_x and CO), Metals and Chemical composition (sulphate, nitrate, EC and OC)	Oil-fired power plant emissions, two secondary nitrates, local gasoline traffic, coal-fired power plant, secondary sulphate, diesel emissions/bus maintenance, Quebec wildfire episode, nucleation, incinerator, airborne soil/road-way dust, and steel plant emissions
Zhou *et al.*[34]	Pittsburgh, USA (urban background)	3–2500	SMPS and APS	$PM_{2.5}$, Gaseous (O_3, NO_x, NO, SO_2 and CO), Metals and Chemical composition (sulphate, nitrate)	Two secondary nitrates, remote traffic, secondary sulphate, lead, diesel traffic, coal-fired power plant, steel mill, nucleation, local traffic, and coke plant.
Kim *et al.*[14]	Seattle, USA (urban background)	20–400	DMPS	Gaseous (NO_x and CO),	Wood burning (48%*), secondary aerosol (21%*), diesel emissions (20%*) and motor vehicle emissions (11%*)
Zhou *et al.*[35]	Pittsburgh, USA (urban background)	3–2500	SMPS and APS	$PM_{2.5}$, Gaseous (O_3, NO, NO_x, SO_2 and CO) and Chemical composition (sulphate, OC and EC).	Sparse nucleation (28.2%), local traffic (21.7%), stationary combustion (21.1%), grown particles and remote traffic (20%) and secondary aerosol (9%)

Note: *Contributions to particle volume concentration. SMPS = Scanning mobility spectrometer; UDMA = Ultrafine differential mobility analyser; UCPC = Ultrafine condensation particle counter; APS = Aerodynamic particle sizer; OPC = Optical particle counter; MAS = Mobile aerosol spectrometer (comprising a combination of differential mobility spectrometer, DMPS, and an optical laser aerosol spectrometer); EEPS = Engine exhaust particle spectrometer.

Table 2: Hourly Pearson product-moment correlations, along with the significance level (p-value), between each factor contribution and measured pollutants (PM_{10}, O_3, NO_x, SO_2 and CO).

	Factor 1	Factor 2	Factor 3	Factor 4	Factor 5	Factor 6
PM_{10}	0.39[a]	0.71[a]	–0.10[a]	–0.15[a]	–0.16[a]	0.31[a]
O_3	–0.14[a]	0.03[b]	–0.15[a]	–0.39[a]	–0.49[a]	0.14[a]
NO_x	–0.04[a]	–0.11[a]	0.37[a]	0.30[a]	0.54[a]	0.01
SO_2	–0.04[a]	–0.04[a]	0.31[a]	–0.05[a]	0.05[a]	0.19[a]
CO	–0.13[a]	0.01	0.23[a]	0.07[a]	0.23[a]	0.02

[a]Correlation is significant at the 0.01 level. [b]Correlation is significant at the 0.05 level.

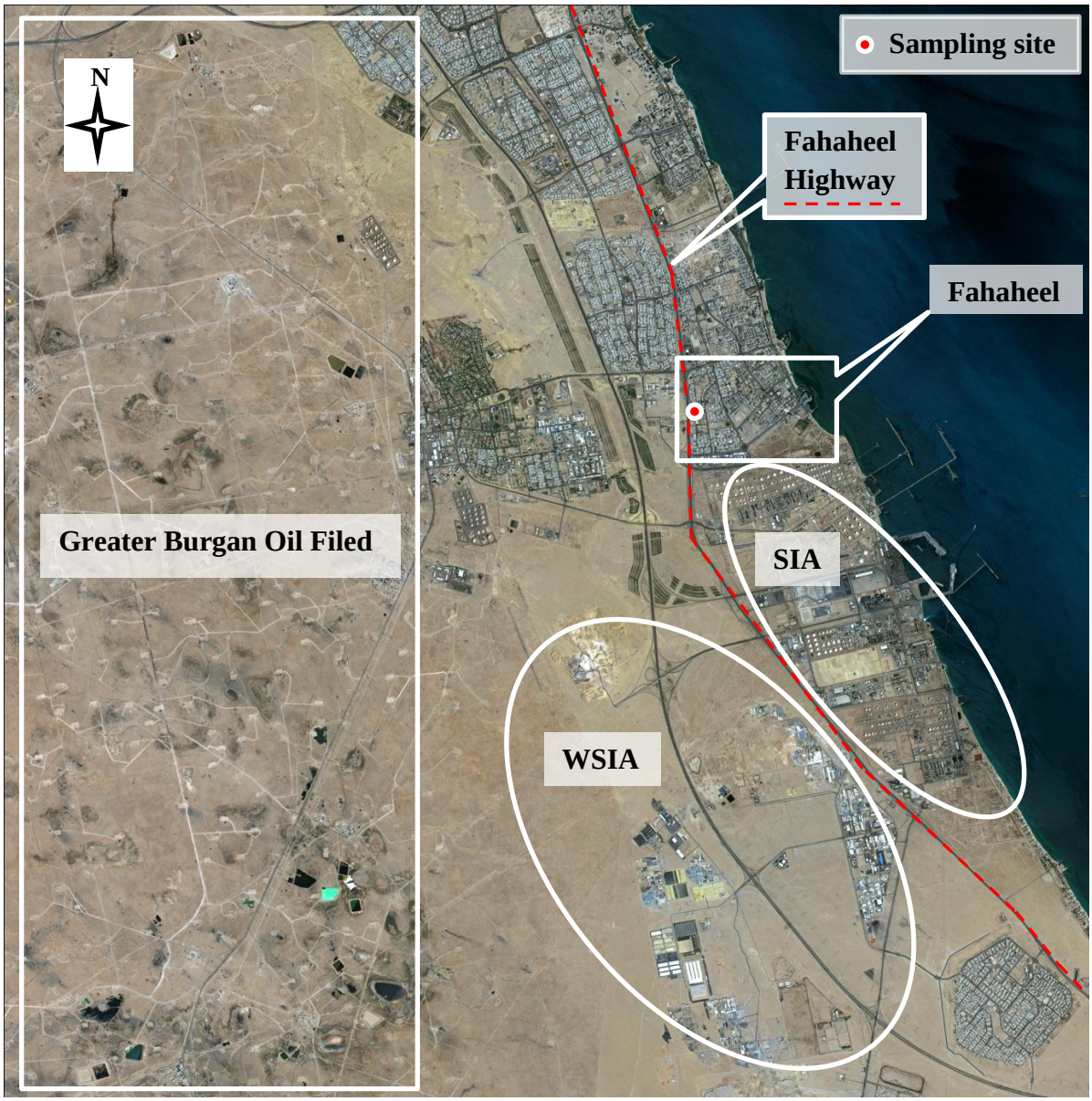

Figure 1

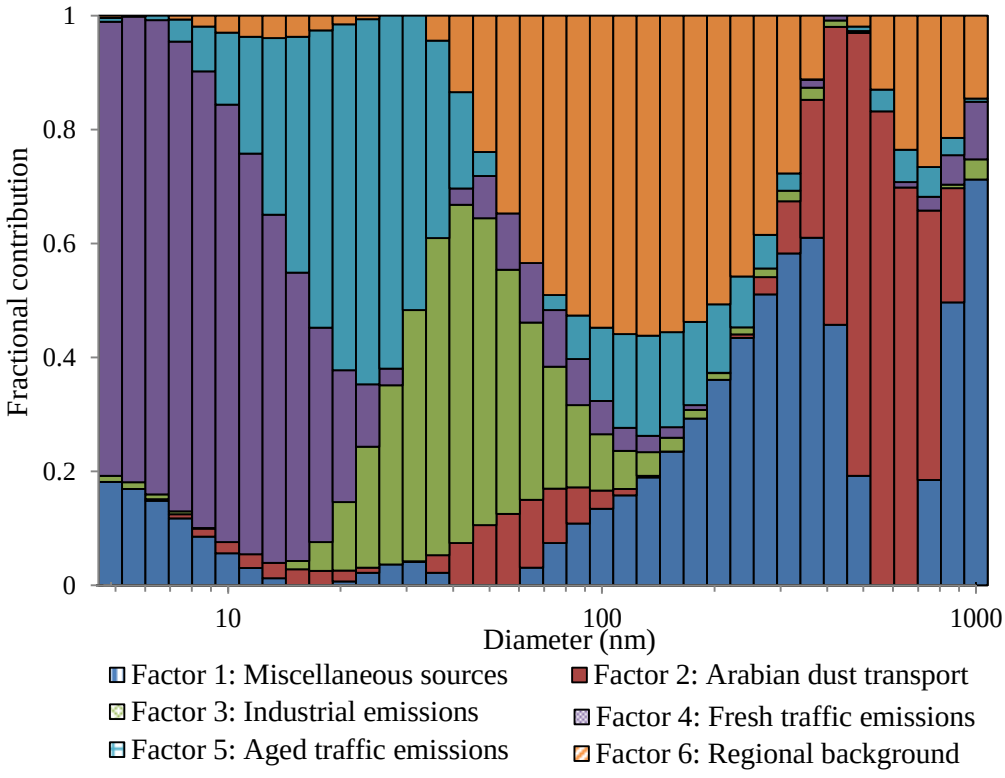

Figure 2

Figure 3

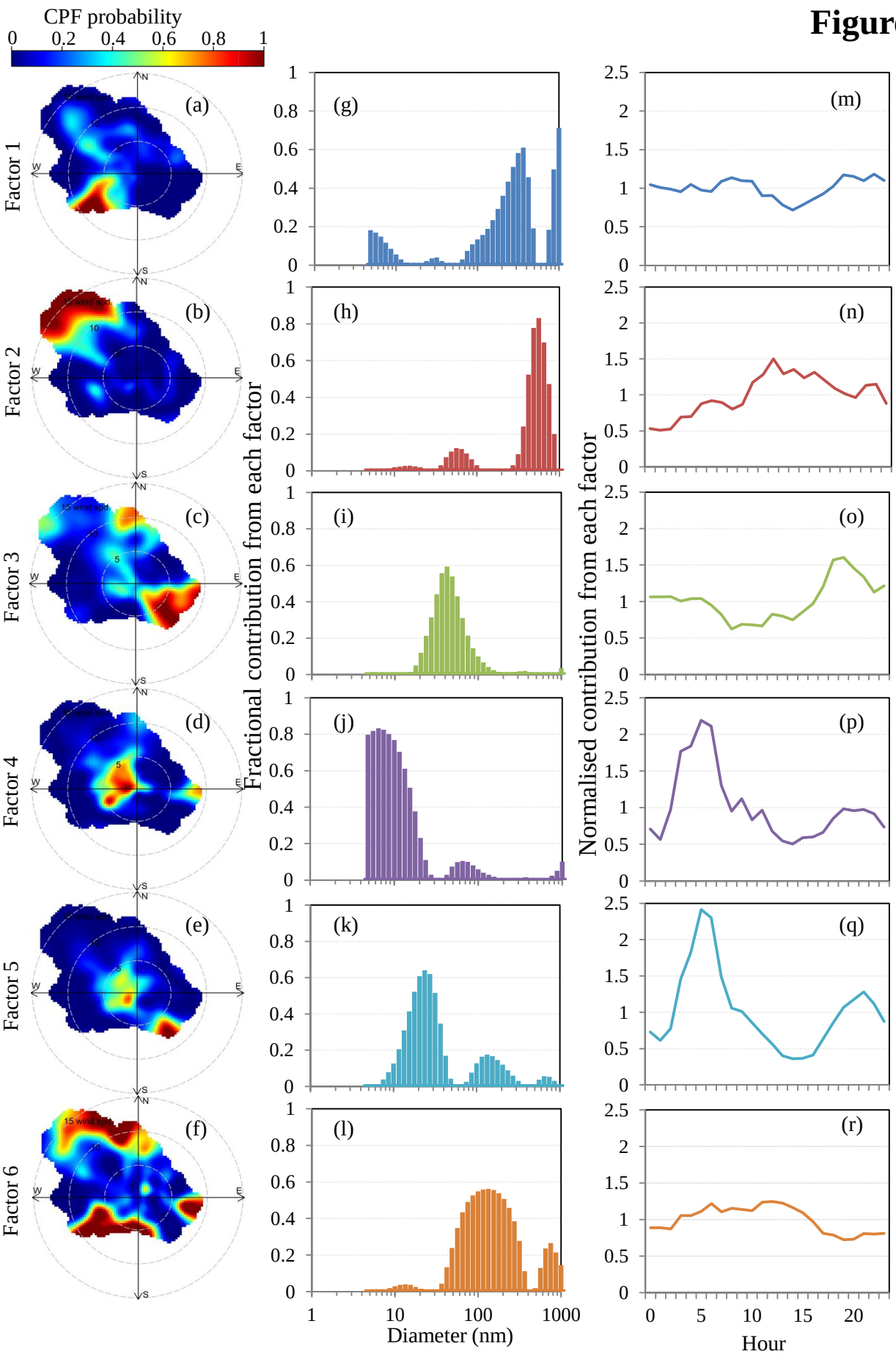

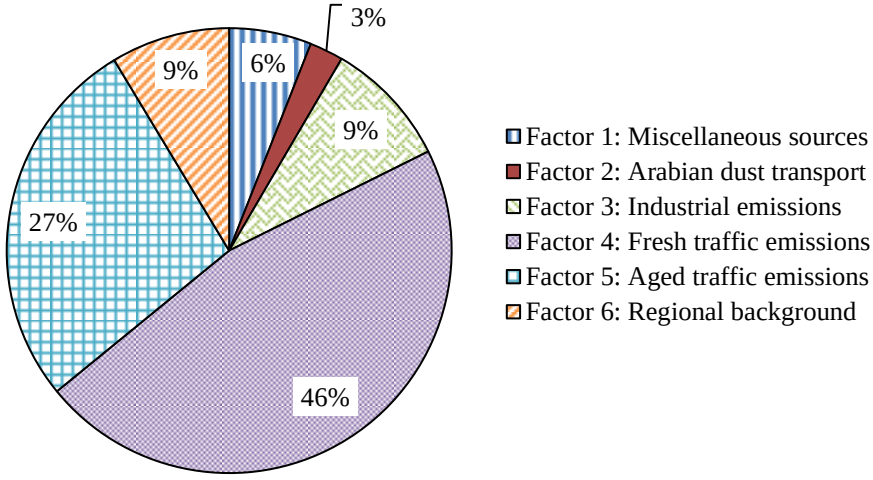

Figure 4

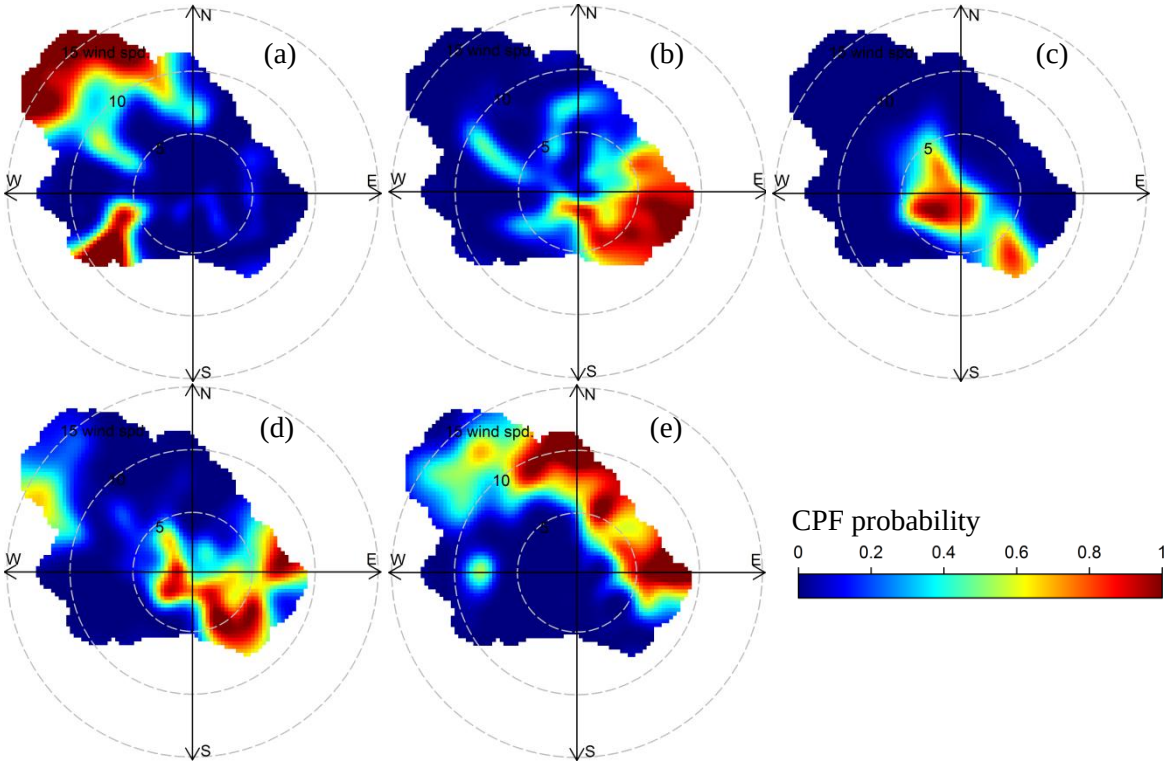

Figure 5